

Identification of defect properties by positron annihilation in Te-doped GaAs after Cu in-diffusion

M. Elsayed* and R. Krause-Rehberg

Martin Luther University Halle, Department of Physics, 06120 Halle, Germany

W. Anwand and M. Butterling

Institut für Strahlenphysik, Helmholtz-Zentrum Dresden-Rossendorf, P.O. Box 510119, 01314 Dresden, Germany

B. Korff

Helmholtz-Institut für Strahlen- und Kernphysik der Rheinischen Friedrich-Wilhelms-Bonn University, 53115 Bonn, Germany

(Received 22 December 2010; revised manuscript received 11 November 2011; published 28 November 2011)

Positron lifetime measurements and Doppler-broadening spectroscopy were combined to investigate the defect properties during Cu diffusion in Te-doped GaAs. The diffusion of Cu was performed during an annealing step at 1100 °C under two different arsenic vapor pressures. The samples were quenched into room temperature water. During a subsequent isochronal annealing experiment, it was found that vacancy clusters were generated and grown, and finally they disappeared. The lifetime results show that, in addition to deep positron traps of vacancy type, positron trapping with a lifetime close to the bulk value of 228 ps occurs. The positron lifetime results give direct evidence of positron localization at shallow traps in GaAs:Te. Due to the Cu contamination during the annealing process, the shallow trap is believed to be the $\text{Cu}_{\text{Ga}}^{2-}$ double acceptor. The concentration of shallow traps is determined and found to be in good agreement with the concentration determined by Hall measurement. It decreases up to saturation with increasing annealing. The positron binding energy to these negative nonopen volume trap centers is determined to be 79 meV. It is found to be in agreement with the calculated value. Moreover, coincidence Doppler-broadening spectroscopy shows clearly that Cu atoms are bound in the direct vicinity of the observed vacancy-like defects. Theoretical calculations of momentum distribution predicted that one Cu atom incorporated into a Ga site surrounds the observed open-volume defects.

DOI: [10.1103/PhysRevB.84.195208](https://doi.org/10.1103/PhysRevB.84.195208)

PACS number(s): 61.72.-y, 78.70.Bj, 66.30.J-, 81.05.Ea

I. INTRODUCTION

GaAs as an extremely versatile semiconductor intended for a wide range of electronic devices is one of the most investigated material systems and the most important semiconductor besides silicon. Point defects play a major role on the important properties of semiconductor materials such as GaAs. They reduce the density of free carriers^{1,2} or mediate, e.g. dopant diffusion.³ The detailed microscopic identification of vacancies and vacancy complexes in GaAs was found to be difficult. The theoretical calculations^{4,5} in addition to diffusion studies³ indicate a predominant role of negative Ga vacancies (V_{Ga}) in *n*-doped GaAs. In contrast, a recent calculation showed that also the As vacancy (V_{As}) could be an abundant defect in highly *n*-doped GaAs because of the low value of formation energy.⁶ Furthermore, acceptor-like vacancies with positive donor complexes also are expected owing to Coulomb attraction. Evidence for such complexes is given by photoluminescence,⁷ infrared absorption,¹ and theoretical considerations of the doping behavior.² Si_{Ga} -donor- V_{Ga} complexes on cleavage planes of highly Si-doped GaAs were identified by scanning tunneling microscopy (STM).⁸ But for other *n* dopants, e.g. tellurium, no such direct identification has been obtained so far. Positron annihilation spectroscopy (PAS) has extensively served as a nondestructive probe for open-volume defects in semiconductors.⁹ Open-volume defects (e.g. vacancy-like defects) act as attractive and deep trapping centers for positrons. Positrons trapped in an open-volume defect are accompanied with subsequent changes in their specific annihilation parameters.¹⁰ Because of the reduced electron density in these defects, the trapped positrons have longer lifetimes and a narrower momentum distribution.^{10,11} Positron

annihilation spectroscopy application to semiconductors has successfully led to reliable information on vacancy-related defects, such as their concentration, their energy levels, or charge states.^{12–15} Positron annihilation spectroscopy studies showed the existence of native vacancies in *n*-doped GaAs.^{16,17} However, the positron lifetime measurement alone is not able to identify the defects as a given isolated gallium¹⁸ or arsenic¹⁶ vacancy or as a vacancy-impurity complex.¹⁷ This difficulty can be overcome by performing positron annihilation momentum measurements. The chemical surrounding of the annihilation site can be identified using the high momentum part of the momentum distribution.^{19–22} This is based on the fact that tightly bound core electrons with high momenta retain their element-specific properties. This permits the identification of vacancies and vacancy-impurity complexes, in particular when measurements are compared to theoretical calculations of the momentum distribution.¹⁹

When the positron binding energy to the defects is very small ($\ll 1$ eV), consequently, the positron wave function is weakly localized. These defects are identified as shallow positron traps.²³ The positron annihilation parameters in shallow traps are practically very close to those in defect-free bulk. Due to the weak binding energy, positrons are effectively trapped only at low temperatures. At higher temperatures, they are thermally detrapped. Impurities in semiconductors lead to the formation of shallow levels for electron and holes in the forbidden gap. The long-range Coulomb field around the negative impurities may bind positrons to Rydberg-like states. Their binding energies could be determined by the positron effective mass. The existence of shallow positron traps is not restricted only to negatively charged nonopen volume defects.

Very small open-volume defects may also act as shallow traps related to the small binding energy of the positron to the defect. In metals, dislocation lines^{24–26} and grain boundaries²⁷ have been suggested to act as shallow traps. It has been observed that the *A* center in Si⁹ shows a typical behavior of shallow traps. Some of the difficulties which have been observed in positron annihilation studies in semiconductors could be explained by shallow traps.^{28–31} Positron annihilation was used to study the defects in semi-insulating (SI) GaAs after Cu in-diffusion. It was found that Cu atoms form double acceptors $\text{Cu}_{\text{Ga}}^{2-}$ which act as a positron shallow trap.³²

The coincident detection of both 511-keV gamma quanta from one annihilation event reduces the disturbing background and hence permits the observation of the high-momentum annihilation distribution.^{19–21} Ga vacancies in Si-doped GaAs were observed using coincidence Doppler-broadening spectroscopy (CDBS).³³ However, the experiment could not determine whether the vacancies are isolated or forming a complex because of the expected low contribution of Si_{Ga} donor on the second adjacent site to the annihilation.³³ Consequently, the identification of the impurity-vacancy complexes in GaAs using positron annihilation is still an open question. It is well known that tellurium is incorporated into the As sublattice only.² If coupling with the nearest Ga vacancies occurs, a detectable contribution to the annihilation is expected, allowing for an identification of this complex. Nevertheless, the momentum distribution for the vacancy cannot be unquestionably determined, especially when the fraction of trapped positrons (η) is unknown. Thus, correlated positron lifetime measurements are necessary to obtain η .³⁴ The experimental results are compared with theoretical calculations of the annihilation characteristics to get a reliable interpretation.

Copper is found as an unintentional impurity in most semiconductors. It determines the room temperature carrier concentration and controls the electric properties of GaAs crystals. Cu may be introduced during crystal growth or subsequent processing steps.³⁵ An evidence for this is the fact that Cu is a rapidly diffusing contaminant already at low temperatures. Cu diffuses very fast by interstitial diffusion (kick-out process)³⁶ and exhibits an unusually large diffusion coefficient in many semiconductors. In GaAs, it was found to be as high as $D = 1.1 \times 10^{-5} \text{ cm}^2 \text{ s}^{-1}$ at 500 °C and $D = 1.8 \times 10^{-9} \text{ cm}^2 \text{ s}^{-1}$ at 100 °C.³⁷ In GaAs, Cu has two levels in the band gap and thus a significant influence on electronic properties. Depending on the cooling speed after a diffusion process, the concentration of electrically active Cu atoms is much lower than the total concentration incorporated.^{38,39} This is because of the low solubility of Cu in GaAs at room temperature which is about $1 \times 10^{16} \text{ cm}^{-3}$.³⁶ This electrically active small fraction of the total Cu concentration acts as acceptors, while the portion of Cu that remains electrically inactive forms Cu-Ga precipitates.³⁹ After Cu in-diffusion in SI GaAs, vacancy complexes containing an As vacancy were observed. Coincidence Doppler-broadening spectroscopy showed that Cu is not bound to the observed vacancy complex.³²

Cu in-diffusion in the investigated samples was performed upon annealing the samples at 1100 °C under different As pressure, where the samples were covered with a thin layer of Cu. These Cu pre-introduced samples were subjected to isochronal annealing at ambient conditions, containing no further Cu source, which leads to Cu out-diffusion. Our

positron lifetime results give evidence that, below 300 K, positrons are trapped to open-volume defects (vacancies) as well as at shallow traps with no open volume, which might be Cu acceptors. The concentration of shallow traps is determined and found to be in good agreement with the acceptor concentration found by Hall measurements. Positron localization in Rydberg states around the negative double acceptor Cu in Cu diffused samples is suggested to be responsible for the origin of shallow traps. The presence of shallow traps in *n*-type GaAs was observed earlier.²³ Their origin was suggested to be negative acceptor-like centers, which are residual impurities or native defects.²³ We will show that Cu out-diffusion depends on the in-diffusion conditions, especially on the arsenic vapor pressure during Cu in-diffusion.

These findings indicate the ability of the PAS method for getting more precise information and in determining whether the vacancy is single or forming complexes. It may help in the future for studying the defects in more complicated semiconductors, such as ternary compounds, and predicting the diffusion mechanisms of impurities.

The paper is presented as follows: In the next section, the details of the experimental work are given. Positron lifetime and coincidence Doppler-broadening results are presented in Secs. III and IV, respectively. In Sec. V, the concentration of shallow traps and positron binding energy at them are determined. Sec. VI concludes the paper.

II. EXPERIMENTAL WORK

The investigated samples were cut from Te-doped GaAs crystals grown by the liquid encapsulated Czochralski technique (LEC) ($5 \times 5 \times 0.55 \text{ mm}^3$) containing a carrier concentration of $n = 3.5 \times 10^{17} \text{ cm}^{-3}$. The samples were covered at one side by 35-nm Cu by evaporating it under UHV conditions. This amount of Cu corresponds to a volume concentration of $6 \times 10^{18} \text{ cm}^{-3}$, which is approximately the upper solubility limit of Cu in GaAs at 1100 °C.³⁷ The deposited layer thickness was controlled by a thickness measurement device (frequency shift of a crystal oscillator), which was calibrated before by atomic force microscopy. High-purity copper-free quartz ampoules were used for the Cu diffusing annealing, and pure As (99.999%) was used as an arsenic vapor source. The samples and the arsenic source were sealed in quartz ampoules under high vacuum. A two-zone temperature furnace was used for the diffusion experiment. Annealing was performed for 3 h at 1100 °C (sample temperature). The temperature of the arsenic source was 550 and 740 °C, which corresponds to an As vapor pressure (P_{As}) of 0.2 and 9.68 bar, respectively.⁴⁰ The annealing time was chosen in such a way that a homogeneous Cu concentration was established in the whole sample. This was calculated according to the diffusion coefficient of Cu in GaAs at 1100 °C³⁷

$$D = 0.03 \text{ cm}^2 \text{ s}^{-1} \exp\left(\frac{-0.53 \text{ eV}}{k_B T}\right), \quad (1)$$

where k_B is the Boltzmann constant. The annealing conditions were chosen to maintain arsenic-rich stoichiometry. After annealing, the ampoules were quenched into water at room temperature. According to the solubility, Cu is now at room temperature in oversaturated state. Thus, Cu atoms have the

tendency to leave the lattice and start out-diffusion, e.g. by forming precipitates. Hall-effect measurements were applied to measure the samples in the as-quenched state. Thereafter, the samples were isochronally annealed in the temperature range up to 900 K, while they were cooled down slowly after each annealing step. Between the annealing steps, temperature-dependent positron lifetime measurements in the temperature range of 29–500 K were done using a conventional fast-fast coincidence system with a time resolution of 220 ps. The ^{22}Na positron source was sandwiched between two identical 4.5- μm -thick Al foils. Then, it was placed between two identical samples. After source and background corrections, the lifetime spectra were analyzed with one, two, or three exponential components, convoluted with the Gaussian resolution function of the spectrometer. The spectra were analyzed using the LT9 program.^{41,42}

The annihilation momentum distribution was observed by coincidence Doppler-broadening spectroscopy measured at 466 K using two Ge- γ detectors in collinear geometry,²⁰ both with an energy resolution of 1.4 keV at 514 keV of ^{85}Sr .

III. POSITRON LIFETIME RESULTS

A. Sample annealed under 10 bar of P_{As}

In a defect-free crystal, positrons annihilate with a single lifetime τ_b , which we have found to be 228 ps in SI GaAs.^{43–45} After Cu in-diffusion at 1100°C under 10 bar of arsenic vapor pressure, the as-quenched sample showed a decrease of the average lifetime in the low-temperature region ($T < 100$ K) and a saturation level of the average lifetime at 220 ps, which is distinctly lower than the value measured in the bulk SI GaAs (228 ps). That indicates a detection of nonopen volume defects, shallow traps, which tend to trap positrons, reflecting thereby properties very close to the bulk annihilation characteristics of the positrons.^{9,23,32} Then, positrons trapped into shallow traps have a lifetime of $\tau_{st} = 220$ ps (st denotes shallow traps). The behavior of the lifetime as a function of the temperature can then be attributed to thermally assisted positron detrapping from these shallow traps. This is because of the high detrapping rate of positrons from shallow positron traps at elevated temperatures. Figure 1 represents the average positron lifetime vs measurement temperature after different annealing steps performed after Cu in-diffusion under 10 bar of As vapor pressure. A distinct decrease in the average lifetime at low temperatures is clearly seen for all curves as well as a similar temperature behavior. Almost no change was observed in the positron lifetime for the annealing steps up to 500 K. Here, after Cu in-diffusion, the shallow traps must be ionized Cu acceptors. Their concentration is up to $2.2 \times 10^{17} \text{ cm}^{-3}$ according to the Hall-effect measurements. It is observed that the samples are converted to p -type, as shown by the Hall effect. This could be ascribed to the high solubility of Cu in GaAs at 1100°C. During annealing up to 750 K, the average positron lifetime increases strongly up to the value of 275 ps, indicating the existence of vacancy-like defects. With a further increase in the annealing temperature, a huge decrease in the average positron lifetime was observed. With annealing at temperatures higher than 850 K, the vacancy clusters grow, and the distance between them becomes much larger than the positron diffusion length. Finally, their concentration

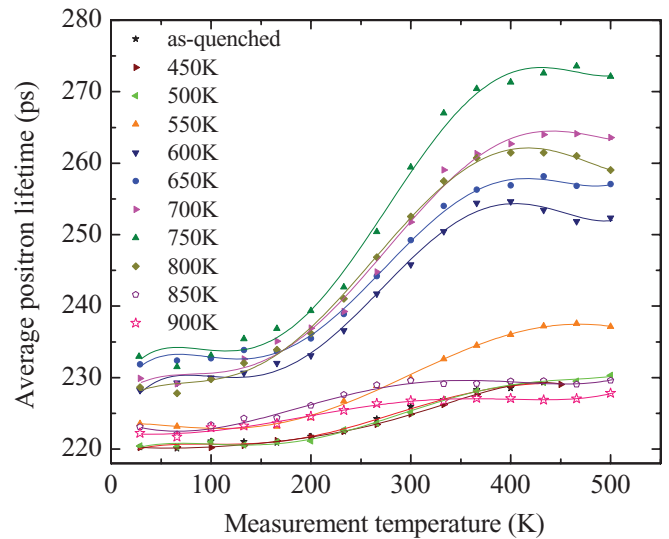


FIG. 1. (Color online) Average positron lifetime as a function of measurement temperature in GaAs:Te for different annealing temperatures. The sample was annealed under 10 bar As vapor pressure.

drops below the sensitivity range of the positrons.^{32,46} The vacancy clusters may also be dissolved, which would lead to a disappearance of the vacancy signal, too. These two possibilities cannot be discriminated by the obtained data alone.

Figure 2 shows the average lifetime and lifetime components and their relative intensities as a function of the annealing temperature. The spectra were measured at 500 K to diminish the effect of shallow traps. It is shown that the open volume of the detected vacancy-type defect increases during annealing. The defect-related lifetime is much higher than that for monovacancies (250–260 ps).⁹ This can only be explained by trapping of positrons at small vacancy clusters. The intensity of the second lifetime component (I_2) increases

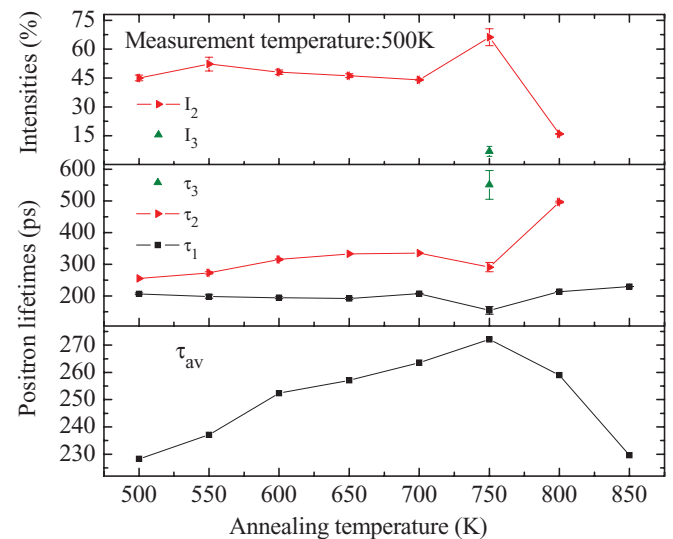


FIG. 2. (Color online) Results of positron lifetime decomposition for different annealing temperatures, each measured at 500 K to avoid the influence of the shallow traps.

with increasing annealing temperature. Only the spectrum measured after annealing at 750 K shows three positron lifetimes. The defect-related lifetime τ_3 reaches the value of 550 ps, corresponding to vacancy clusters with a larger number of vacancies than 15 but with low intensity I_3 . Here, τ_1 is always less than the bulk lifetime, which indicates that no saturation trapping takes places in the open-volume defects.

The positron trapping rate κ_d is proportional to the defect concentration C_d and is expressed as:

$$\kappa_d = \mu C_d. \quad (2)$$

Here, μ is the trapping coefficient. For a two-component decomposition, i.e. only one dominating defect type, the trapping rate is given by:

$$\kappa_d = \frac{1}{\tau_b} \frac{\tau_{av} - \tau_b}{\tau_d - \tau_{av}}. \quad (3)$$

In the case of two noninteracting deep positron traps, the lifetime spectrum has three exponential decay components. It follows for the trapping rates:

$$\kappa_{d1} = I_2(\lambda_1 - \lambda_2), \quad \kappa_{d2} = I_3(\lambda_1 - \lambda_3), \quad (4)$$

where κ_{d1} is the positron trapping rate to the first defect and κ_{d2} is that to the second defect type.

The annihilation fractions (η_i) are also expressed as:

$$\eta_2 = \frac{\kappa_{d1} \tau_b}{1 + \tau_b(\kappa_{d1} + \kappa_{d2})} = \frac{\kappa_{d1}}{\lambda_b + \kappa_{d1} + \kappa_{d2}}, \quad (5)$$

$$\eta_3 = \frac{\kappa_{d2} \tau_b}{1 + \tau_b(\kappa_{d1} + \kappa_{d2})} = \frac{\kappa_{d2}}{\lambda_b + \kappa_{d1} + \kappa_{d2}}.$$

Because the average lifetime can be experimentally determined with high accuracy, the trapping rate is often expressed in terms of τ_{av} by Eq. (3). Here, μ is taken as 10^{15} s^{-1} at 300 K and $0.9 \times 10^{15} \text{ s}^{-1}$ at 500 K,^{47,48} τ_b is the bulk lifetime (228 ps), τ_{av} is the average positron lifetime, calculated from the experimental lifetime components according to Eq. (3), and τ_d is the defect-related lifetime. The trapping rates are determined using Eqs. (3) and (4) for two and three lifetime component spectra, respectively. The defect concentration is calculated by applying Eq. (2). The lower panel of Fig. 3 represents the defect concentration vs the annealing temperature, where the defect concentration increases from $2.2 \times 10^{15} \text{ cm}^{-3}$ at 500 K up to $9.4 \times 10^{16} \text{ cm}^{-3}$ at 750 K. For further annealing temperatures, the defect density decreases due to the decrease of the average positron lifetime.

The number of vacancies in a cluster (N) is estimated from the defect-related lifetime according to the calculation in Ref. 49, which is based on the superimposed-atom model by Puska and Nieminen.⁵⁰ As shown in the upper panel of Fig. 3, the number of vacancies in a cluster increases from one at annealing temperature of 500 K to four vacancies at 700 K of the annealing temperature. At further annealing temperature, at 750 K, the defect-related lifetime is 550 ps, which corresponds to a cluster of >15 vacancies (not indicated in Fig. 3). This value of lifetime is roughly theoretically estimated as a cluster of >50 vacancies. The positron lifetime measurements for the sample annealed under 10 bar of P_{As} (Fig. 1) show a maximum effect after annealing at 750 K. The lifetime decomposition is represented in Fig. 4. In the low-temperature region ($T < 100 \text{ K}$), the 260-ps component was fixed. The positron lifetime

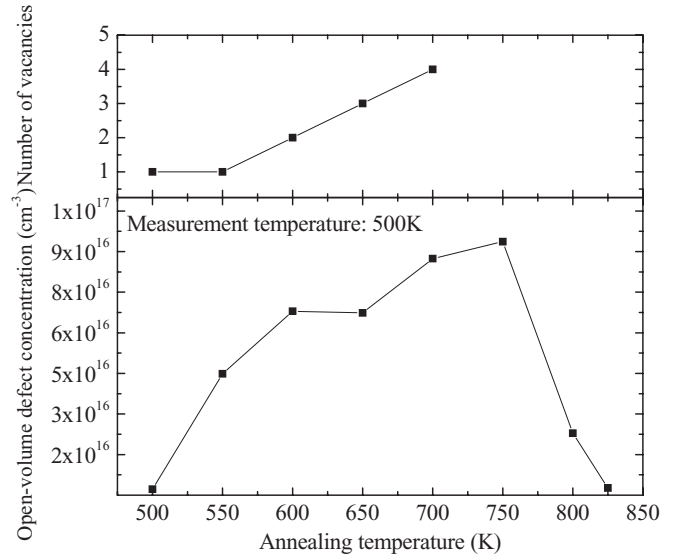


FIG. 3. Defect concentration and the number of vacancies N included in one cluster vs the annealing temperature in Cu-diffused GaAs:Te calculated from the positron lifetime results in Fig. 1.

τ_2 increases with increasing measurement temperature up to 300 K. For a further temperature increase, three-component decomposition is predominant with $\tau_3 \approx 600 \pm 35 \text{ ps}$ (the lower panel of Fig. 4). This indicates the generation of vacancy cluster with $N > 50$ vacancies. The value of τ_2 oscillates around 290 ps (monovacancy) with an intensity I_2 of 66 %. Here, I_3 increases with the temperature to 7% (upper panel of Fig. 4). The positron annihilation fraction (η_2, η_3) for the defect-related lifetimes is estimated using Eq. (5) and illustrated in Fig. 5. It is found that the annihilation fraction of the second component increases with the temperature and reaches 0.35 due to the increase in the trapping rate. Further, η_3 only increases to 0.05, which indicates the low value of the trapped positrons fraction to the vacancy clusters.

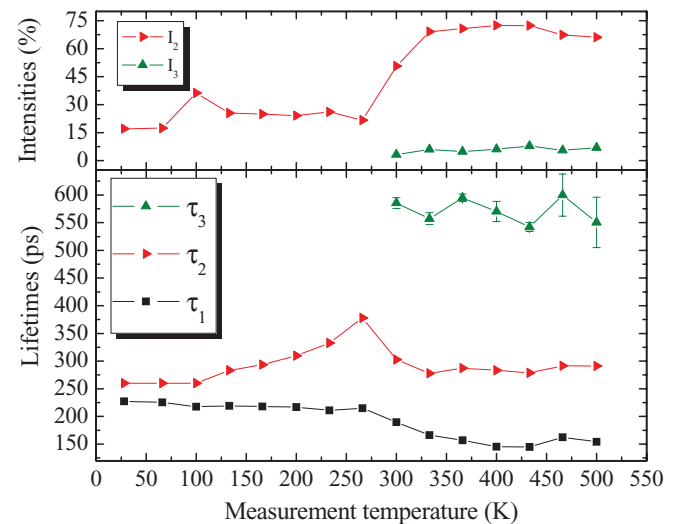


FIG. 4. (Color online) Positron lifetime decomposition of the isochronally annealed sample at 750 K as a function of measurement temperature.

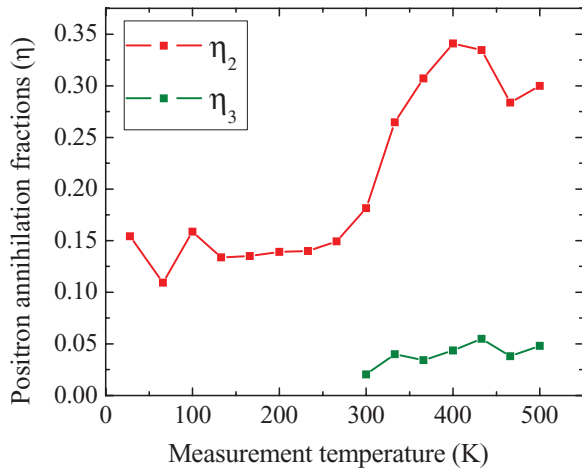


FIG. 5. (Color online) Positron annihilation fraction vs the measurement temperature calculated using the lifetime decomposition presented in Fig. 4.

Due to the steep decrease in the positron lifetime after annealing the sample at 850 K (Fig. 1), another GaAs:Te sample was treated under the same conditions and annealed up to 825 K to see the effect on the longer lifetime component. Then, the temperature-dependent positron lifetime measurement is performed, as shown in Fig. 6. The average lifetime increases from 224 ps in the low temperature region ($T < 100$ K) to 234 ps at $T > 300$ K. It was found that the value of τ_1 at $T > 300$ exceeds that of the bulk lifetime, which reflects a complete trapping of positrons. It is important to note that the defect-related lifetime τ_2 reaches values as high as 750 ps but with low intensity $\sim 1\%$ (the upper two panels of Fig. 6). This supports the assumption that the vacancy clusters grow, and their density decreases. During further annealing, the lifetime decreases, and the vacancy signal disappears (Fig. 1). It was assumed that the small clusters combine to each other forming

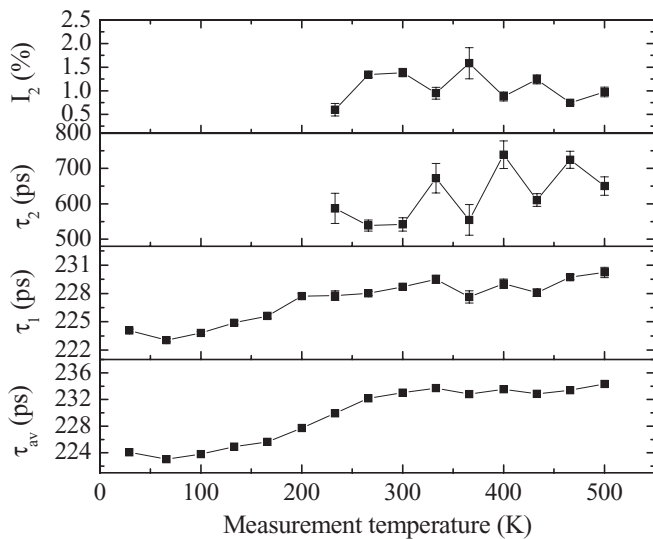


FIG. 6. Positron lifetime decomposition at 825 K of the isochronally annealed sample as a function of measurement temperature.

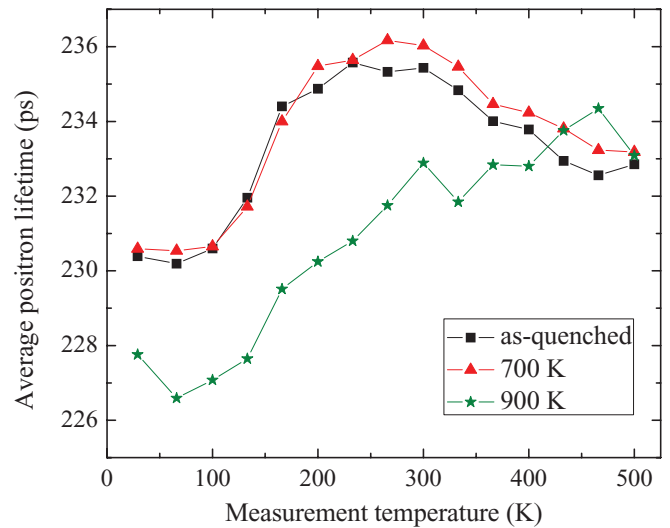


FIG. 7. (Color online) Average positron lifetime as a function of measurement temperature in GaAs:Te without Cu.

large voids with a distance between them being so large that they are not seen by positron any more.⁴⁶

The results above are compared to those obtained for a sample annealed under very similar conditions which was not treated with Cu in order to demonstrate the effect of Cu. As illustrated in Fig. 7, the as-quenched sample shows a higher value of the average lifetime (236 ps), which is very small compared to the Cu-diffused sample (275 ps after annealing at 750 K). This can be explained by trapping of positrons in vacancies. The decrease of the lifetime in the low-temperature region is ascribed to the positron trapping into shallow traps. The shallow traps are attributed to intrinsic defects (e.g. $\text{Ga}_{\text{As}}^{2-}$)⁵¹ or extrinsic defects.⁴⁸

Here, τ_{av} decreases slightly with increasing the annealing temperature in the temperature range up to 400 K, while at 500 K, the average lifetime is almost the same, which can be attributed to the diffusion of shallow traps. In contrast, in the case of the GaAs:Te after Cu in-diffusion (Fig. 1), almost no change in the average positron lifetime was detected in the as-quenched state. However, during the annealing steps until 750 K, the average positron lifetime increases strongly, and at annealing temperatures higher than 850 K, the vacancy cluster signal almost disappears. This indicates that the observed vacancy-like defects in the Cu-diffused sample are Cu-induced.

B. Sample annealed under 0.2 bar

To show the effect of the As vapor pressure, another sample was annealed at 1100 °C under 0.2 bar of P_{As} . Figure 8 presents the average lifetime as a function of the sample temperature after different annealing steps performed after in-diffusion of $6 \times 10^{18} \text{ cm}^{-3}$ Cu atoms at 1100 °C under 0.2 bar of arsenic vapor pressure (As temperature is 550 °C). The lifetime measurement of the as-quenched sample shows no positron trapping in open-volume defects. The average lifetime in the high-temperature region is very close to the bulk lifetime in SI GaAs (228 ps). As the temperature decreases, the lifetime decreases, which is a typical dependence for shallow traps. This is clearly shown for all curves. Almost no change was

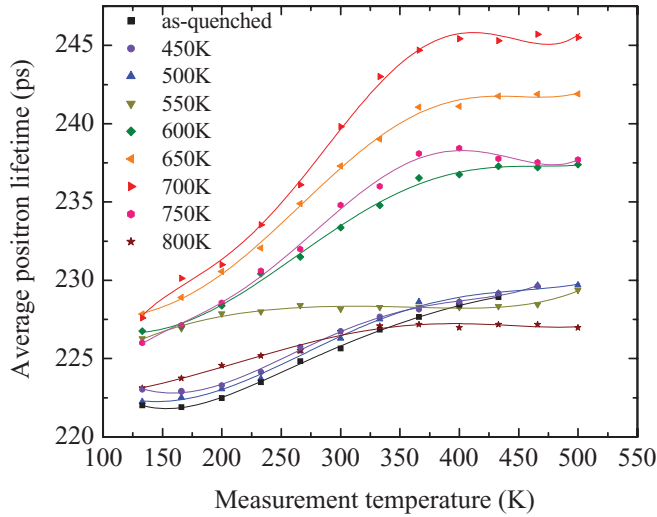


FIG. 8. (Color online) Average positron lifetime as a function of measurement temperature in GaAs:Te for different annealing temperatures (0.2 bar of As vapor pressure).

observed for the first annealing steps up to 500 K. As we mentioned above, for the Cu-diffused sample, the shallow traps should be ionized Cu acceptors. In the course of annealing up to 700 K, the average positron lifetime increases and reaches 246 ps, indicating the detection of vacancy-like defects. This lifetime value is much lower than that in the case of the Cu-diffused sample under 10 bar of P_{As} , 275 ps (Fig. 1). With an additional increase in the annealing temperature, a rapid decrease in the average positron lifetime was observed. Figure 9 shows the positron lifetimes and the intensity of the defect-related lifetime I_2 vs the annealing temperature for GaAs:Te. The spectra were measured at 500 K to avoid the effect of shallow traps. The spectra measured after the first annealing steps up to 550 K show only one lifetime very close to the bulk lifetime. At annealing temperatures higher than 550 K, the spectra show two-component decomposition with

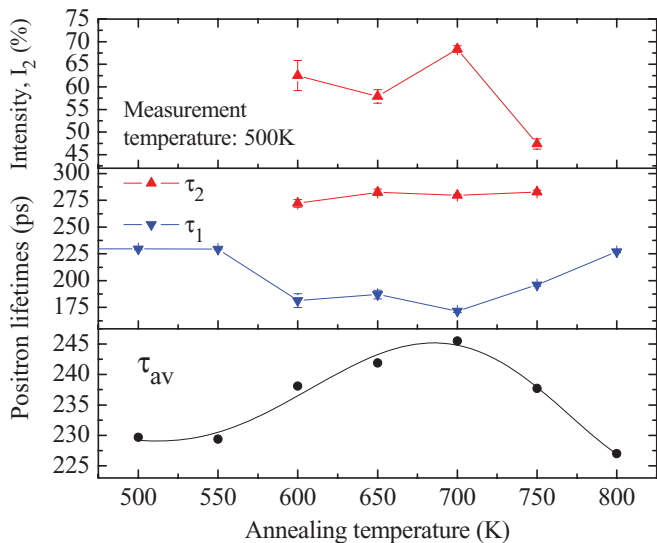


FIG. 9. (Color online) Results of positron lifetime decomposition for different annealing temperatures, each measured at 500 K (0.2 bar As vapor pressure).

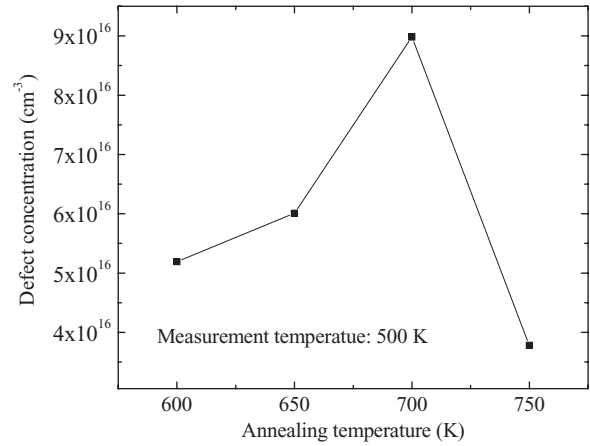


FIG. 10. Defect concentration vs the annealing temperature in Cu-diffused GaAs:Te under 0.2 bar of As vapor pressure. These data were estimated using the positron lifetime results presented in Fig. 9.

$\tau_2 = 280 \pm 3$ ps, which lies in the monovacancy region.⁴⁹ It is much lower than the divacancy value of 332 ps.⁹ Thereafter, the number of vacancies in the annealing temperature range (600–750 K) is estimated to be only one vacancy. The intensity of the second component is presented in the upper panel of Fig. 9. Here, I_2 increases from 60% at 600 K to 68% at 700 K then decreases for higher annealing temperatures. Because the intensity of the defect-related lifetime is proportional to the defect concentration, this high value of I_2 leads to a higher number of defects. Figure 10 illustrates the defect density against the annealing temperature. The defect concentration is calculated from the lifetime decomposition according to Eq. (2). It increases from $5.2 \times 10^{16} \text{ cm}^{-3}$ at 600 K to $9 \times 10^{16} \text{ cm}^{-3}$ at 700 K of annealing temperature. At 750 K, the defect concentration decreases to $3.8 \times 10^{16} \text{ cm}^{-3}$.

We have calculated the positron lifetime for different defects and for V_{Ga} surrounded with different numbers of Cu atoms for an unrelaxed structure in GaAs using atomic superposition method,^{34,50} as tabulated in Table I. It is clearly shown that, with the increasing number of Cu atoms around the V_{Ga} , the lifetime increases. The experimentally observed lifetime (280 ps) is higher than the theoretically calculated lifetime value of the isolated V_{Ga} (267 ps) but less than that of V_{Ga} decorated with 2 Cu atoms (283 ps). Thus, it is more probable that the detected defect is V_{Ga} -1Cu_{Ga} complex (276 ps). Coincidence Doppler-broadening measurements support this assumption, as shown in the next section.

TABLE I. Theoretically calculated positron lifetime for different vacancies and vacancy complexes in GaAs for unrelaxed structure.

| Vacancy | Lifetime (ps) |
|-----------------------------|---------------|
| GaAs bulk | 232 |
| $V_{Ga}V_{As}$ | 332 |
| V_{Ga} | 267 |
| V_{Ga} -1Cu _{Ga} | 276 |
| V_{Ga} -2Cu _{Ga} | 283 |
| V_{Ga} -3Cu _{Ga} | 291 |
| V_{Ga} -4Cu _{Ga} | 298 |

IV. RESULTS OF COINCIDENCE DOPPLER-BROADENING MEASUREMENTS

Due to the high solubility and high diffusivity of copper in GaAs, it was assumed that these vacancy clusters are decorated by Cu precipitates.^{44,46} Coincidence Doppler-broadening spectroscopy measurements were done to confirm whether the observed vacancy-like defects were surrounded by Cu atoms. The most important parameter is the shape of the high-momentum distribution indicated by the W parameter, which is responsive to the chemical surroundings of the annihilation site. The results of coincidence Doppler-broadening measurements are shown in the left part of Fig. 11. The spectra measured at 466 K, normalized to an undoped SI GaAs reference sample, show no positron trapping. In panel (a) of Fig. 11, the ratio curve of annihilation momentum distribution obtained in pure copper is shown. In panel (b), two samples are measured, GaAs:Te diffused with Cu under 0.2 bar then annealed up to 700 K, and Cu diffused GaAs:Te under 10 bar annealed up to 750 K. If positrons annihilate with core electrons of copper, the intensity in the high-momentum distribution area of the Doppler peak at $(7-20) \times 10^{-3} m_0 c$ is higher than in bulk GaAs (ratio is larger than one, panel (a) of Fig. 11). Thus, the existence of Cu atoms in the immediate neighborhood of a positron trap can be seen as such a distinct increase of the intensity of the electron momentum distribution. Cu being incorporated on the Ga sublattice is an adjacent neighbor to vacancy-like defects and thus must be perfectly observed at the high momentum part of the CDBS spectrum. The ratio curves of both annealed samples show a clear sign that Cu atoms are in the vicinity of the detected vacancies. This is because the shape of momentum distribution for both annealed GaAs:Te samples is very similar to the spectrum of pure Cu. Consequently, the results of the high momentum part of annihilation momentum distribution for the Cu-diffused GaAs:Te are determined by the annihilation of positrons with the core electrons of Cu atoms.^{46,52} These

results show clearly that the observed vacancy-like defects are decorated with copper. The presence of such cluster-Cu precipitate complexes was observed by transmission electron microscopy (TEM).⁴⁶

Theoretical calculations of the annihilation momentum distribution were performed to support our experimental findings. These calculations were done using the method introduced in Refs 19 and 34, which is found to give momentum distribution and positron lifetime in GaAs in sufficient agreement with the experiment.³⁴ The momentum distribution is calculated via the free atomic wave functions within the model of the independent particles for each core electron state. The final momentum distribution is given by taking the summation of the contributions from each state weighted by the partial annihilation rates calculated within the generalized gradient approximation (GGA) of positron annihilation.⁵³ Lattice relaxation was not taken into account within the calculations. The momentum distribution of Cu is calculated and represented as a ratio to the bulk GaAs in Fig. 11, panel (c). It is clearly shown that theoretically calculated and measured momentum distributions are in reasonable agreement. The theoretically calculated momentum distributions for V_{Ga} , V_{As} , the divacancy, and for different possibilities of surrounding them by Cu atoms in GaAs (normalized to the bulk distribution) are shown in panel (d) of Fig. 11. A probable shift in the calculated curves is due to the approximation and unrelaxed coordinates. It is clearly shown in the calculated curves that, with increasing of vacancy bound Cu atoms, the ratio of the curves also increases. This agrees with the assumption of the presence of Cu in the immediate vicinity of the observed vacancy-like defects. The momentum distribution curve for the V_{Ga} surrounded by one Cu atom incorporated into the Ga sublattice ($V_{\text{Ga}}\text{-Cu}_{\text{Ga}}$) is very close to the experimental curves of the annealed samples under 0.2 and 10 bar of P_{As} . Thus, we conclude that the detected defect is a $V_{\text{Ga}}\text{-1 Cu}_{\text{Ga}}$ complex.

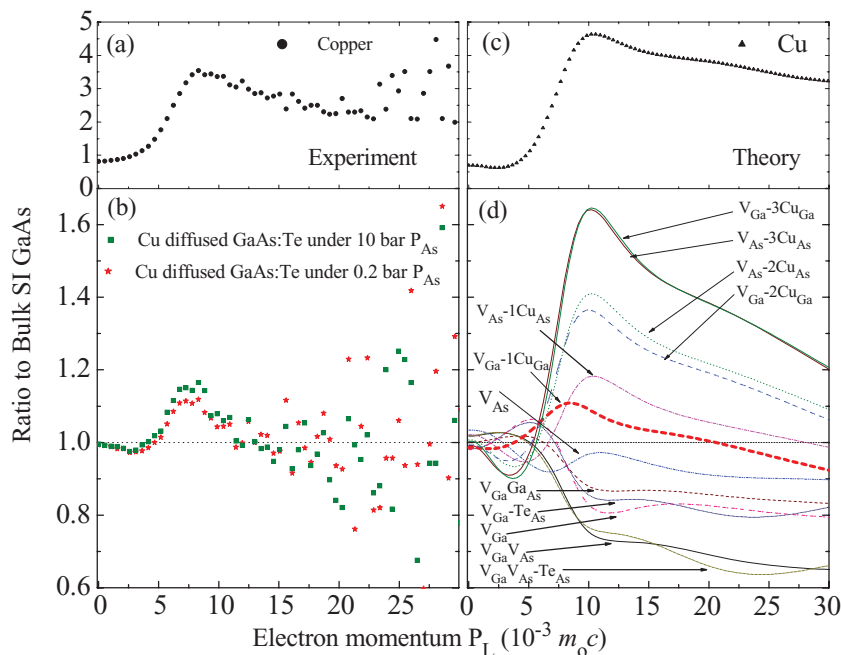


FIG. 11. (Color online) High momentum part of the positron annihilation momentum distribution, normalized to SI undoped GaAs reference (left part). (a) In the upper part, the spectrum for pure copper is shown. (b) The lower part represents spectra of two GaAs:Te samples: In one of them, the Cu in-diffusion is performed under 0.2 bar of P_{As} and annealed subsequently up to 700 K. For the other, the Cu in-diffusion is carried out under 10 bar of P_{As} , and the sample is subject to isochronal annealing up to 750 K. The right part shows the ratio of high momentum distribution to the bulk GaAs for (c) pure Cu and (d) different vacancies in GaAs from theoretical calculations. The calculation was done using GGA. The curve of the $V_{\text{Ga}}\text{-Cu}_{\text{Ga}}$ complex is highlighted to emphasize the agreement to the respective experimental data in GaAs:Te annealed samples.

V. DETERMINATION OF CONCENTRATION OF SHALLOW TRAPS AND POSITRON BINDING ENERGY

The decrease of the average lifetime in the low-temperature region is direct evidence for the existence of shallow positron traps. Furthermore, positron diffusion length experiments were used as a direct probe for shallow traps.²³ A decrease in the positron diffusion length was observed between 100–200 K, and this was accompanied with changes in the positron lifetimes at the same temperature range. This was ascribed to thermal positron detrapping from the shallow traps.²³ Positrons getting trapped to the shallow traps have a lifetime very close to those of the bulk, which results in difficulties for the determination of the detailed microscopic structure of the shallow traps. This is because these traps are not of vacancy type and do not involve open volume. Negatively charged ions can induce the observed shallow positron state. In the samples under investigation, after Cu diffusion, Cu double acceptors act as shallow trap centers.³² It was suggested that residual impurities (e.g. C_{As}^-) and native defects, such as gallium antisite, Ga_{As}^- , are responsible for the formation of negative centers acting as shallow traps for positrons in undoped GaAs.^{23,54} To estimate the concentration of shallow traps, the one- and two-defect-type trapping models were used. At the first annealing steps up to 500 K, the decomposition of the lifetime spectra shows only one component in the whole temperature range. For these annealing steps, one defect type model is used to determine the trapping rate at 29 K, where $\tau_d = \tau_{st} = 220$ ps is assumed. As mentioned above, this lifetime value is observed in the as-quenched sample. The trapping rate for shallow traps can then be calculated by applying Eq. (3). Using Eq. (2), the concentration of shallow traps can be determined. A trapping coefficient $\mu = 5 \times 10^{16} \text{ s}^{-1}$ is applied.⁹ At annealing temperatures higher than 550 K, the spectra consist of two lifetime components, especially in the high-temperature region, which indicates the detection of vacancy-like defects as well as shallow traps which are effective only at low temperature. Thus, the model of two defect types should be used. The positron trapping rate to vacancies is estimated in the high-temperature region (where no effect of shallow traps is expected). Then the trapping rate to shallow traps at 29 K could be calculated. The estimated concentration of the shallow traps vs the annealing temperature is shown in Fig. 12. It is found that the value estimated at the annealing temperature of 450 K is very close to that measured using Hall measurement ($2.2 \times 10^{17} \text{ cm}^{-3}$). With increasing the annealing temperature, the concentration of shallow traps decreases and saturates at 10^{16} cm^{-3} . After Cu in-diffusion, Cu is in an oversaturated state according to the solubility. With annealing, Cu atoms have the propensity to leave their lattice sites and start the out-diffusion, e.g. forming precipitates. This results in a decrease of the electrically active fraction of Cu, i.e. a decrease of the concentration of the acceptors and thus shallow traps.

The ratio of the detrapping (δ) and trapping rates is given by the thermodynamic approach to detrapping of positrons from the defect⁵⁵ as,

$$\frac{\delta}{\kappa_{st}} = \frac{1}{C_{st}} \left[\frac{m^*}{2\pi\hbar} \right]^{3/2} (k_B T)^{3/2} \exp \left[\frac{E_b}{k_B T} \right], \quad (6)$$

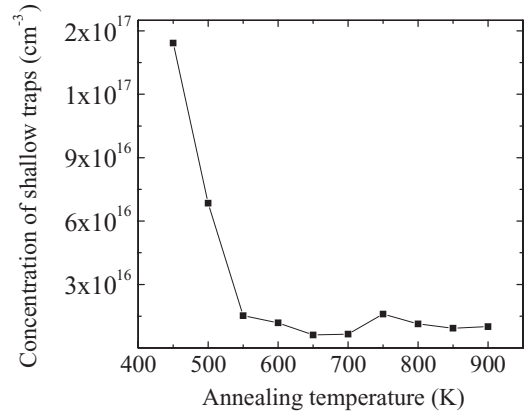


FIG. 12. The concentration of shallow positron traps determined at 29 K as a function of the annealing temperature in Cu-diffused GaAs:Te annealed under 10 bar of P_{As} .

where E_b is the positron binding energy to the shallow traps with the concentration C_{st} and m^* (positron effective mass). Equation (6) is fitted to the experimental data, after the corresponding trapping equations are solved to determine the transition rates δ and κ_{st} . We have applied the three-state trapping model, which consists of positron annihilation in the free state, trapping to vacancy-like defects with κ_v and trapping to shallow traps with κ_{st} and detrapping from shallow traps with δ . An experimental formula for positron detrapping transition is given by the solution of the kinetic trapping equation:⁵⁶

$$\frac{\delta}{\kappa_{st}} = \left[\frac{I_2}{I_1\kappa_v - I_2(\lambda_b - \lambda_2)} - \frac{1}{\kappa_{st}} \right] (\lambda_{st} - \lambda_2), \quad (7)$$

where $\tau_2 = \lambda_2^{-1}$ is the lifetime of the longest component in the lifetime spectrum, which has the intensity I_2 . Here, $\lambda_b = \tau_b^{-1} = (228 \text{ ps})^{-1}$ is the annihilation rate in the bulk crystal. We assumed $\lambda_{st} = \tau_{st}^{-1} = (220 \text{ ps})^{-1}$. In order to obtain the experimental detrapping rate using Eq. (7), information on the temperature dependencies of κ_v and κ_{st} is needed. The simultaneous determination of three parameters κ_v , κ_{st} , and δ from the experimental data is impossible. This was simplified by assuming that the trapping rates κ_v and κ_{st} do not depend on the temperature.²³ The value of κ_v is evaluated at high temperature, $T > 400$ K (where no positron trapping to shallow traps and the lifetime is saturated). Here, κ_{st} is estimated at very low temperature, close to 0 K (no thermal detrapping). Equation (7) shows that the detrapping rate is totally governed by the intensity of the vacancy component I_2 .

Figure 13 shows the Arrhenius plot of the measured detrapping rates from Eq. (7) in Cu-diffused GaAs:Te annealed under 10 bar of P_{As} determined from the decomposition of positron annihilation lifetime spectra measured after annealing at 650 K. The solid line in Fig. 13 represents the fit of Eq. (6) to the experimental data. The slope yields a binding energy of $(79.4 \pm 6) \text{ meV}$. The detrapping rate is noticed to agree with the trapping rate ($\kappa_{st} = \delta$) at 166 K. All the lifetime spectra measured after annealing the sample at 650 K show two-component decomposition, but the decomposition below 100 K is not so reliable. Thus, a 255-ps component is fixed to reduce the statistical uncertainties of the fitting. The positron,

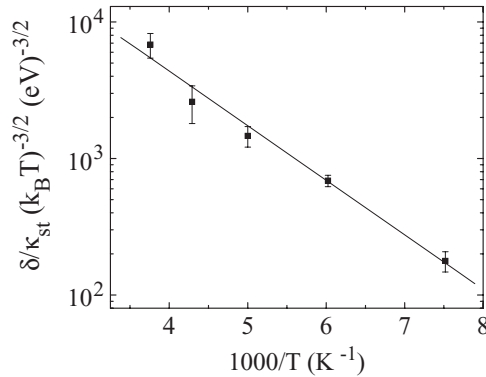


FIG. 13. The ratio of the detrapping and trapping rates in Cu-diffused GaAs:Te annealed under 10 bar of P_{As} calculated from the decomposition of the lifetime spectra after annealing the sample at 650 K. The solid line is the fit to the experimental data with $E_b = 79.4$ meV.

as a positively charged particle, can get localized into the Rydberg states of a Coulomb field around these centers. The binding energy of the positron to these states can be estimated using a simple formula:^{23,57}

$$E_b = \frac{13.6 \text{ eV}}{\varepsilon^2} \left[\frac{m^*}{m_e} \right] \frac{1}{n^2}, \quad (8)$$

where ε is the dielectric constant of the material ($\varepsilon = 12.9$ in GaAs), m^* is the positron effective mass, m_e is the rest mass of electron, and n is the quantum number. In all solids, the effective mass of the positron is very close to its free mass ($m^* = m_e$).⁵⁸ A value of $E_b = 81.7$ meV is obtained using Eq. (8) for the binding energy in the first Rydberg state ($n = 1$). It is worth mentioning that our experimentally determined value of binding energy is in excellent agreement with that value calculated by Eq. (8).

Here, E_b is determined for n -type GaAs as (43 ± 5) meV²³ and for GaAs:Te as (60 ± 20) meV.⁵⁹ These earlier results are explained by detrapping of positrons from the excited states, whereas our results indicate that positrons are detrapped from the first state. The trapping coefficient of positrons to the Rydberg states can be estimated using the concentration $2.2 \times 10^{17} \text{ cm}^{-3}$ of ionized acceptor-like centers obtained from the Hall measurement. When the detrapping possibility approaches zero ($T < 100$ K), κ_{st} has a value of $1.63 \times 10^{11} \text{ s}^{-1}$ (for the sample annealed at 450 K). Using Eq. (2), the specific trapping rate is estimated to be $3.2 \times 10^{16} \text{ s}^{-1}$. It is comparable to the large capture rate for positrons at negatively charged vacancies in GaAs.^{9,48} This is not surprising because negatively charged vacancies are surrounded by very similar attractive Coulombic tails.

VI. CONCLUSION

To summarize, in this paper, we have systematically studied positron annihilation in GaAs:Te ($3.5 \times 10^{17} \text{ cm}^{-3}$) after Cu diffusion at 1100°C under two different As vapor pressures (0.2 and 10 bar).

During isochronal annealing, Cu_{Ga} atoms dissolve, leaving their sites (Ga sublattices), and start out-diffusion forming precipitates, which are connected to vacancy clusters. Thus, when Cu atoms leave the Ga sublattice and form precipitates, some open-volume defects must be generated. In the first place, these are V_{Ga} , but because of the observed large defect-related lifetime, vacancies in both sublattices should be comprised. Thereafter, As atoms must leave and precipitate or go into interstitial sites. If so, this process should depend on the stoichiometry, i.e. it depends on the amount of the excess As in GaAs. That is already observed for the samples annealed under different As vapor pressure. The sample annealed under high As vapor pressure showed a defect-related lifetime corresponding to vacancy clusters, whereas that annealed under low P_{As} showed a defect-related lifetime corresponding to monovacancies. Thus, the higher the As vapor pressure during Cu in-diffusion is, the easier the As atoms precipitate, and the more pronounced is the course of void formation. The Ga vacancy concentration increases with increasing P_{As} . Thus, in order to keep the crystal stoichiometry, As vacancies should be emitted, then collapse and agglomerate with Ga vacancies forming vacancy clusters.

The behavior of the temperature-dependent average positron lifetime can be attributed to thermally assisted positron detrapping from these shallow traps. The Cu content explained the observation of shallow traps. Cu ionized acceptors ($\text{Cu}_{\text{Ga}}^{2-}$) act as the observed shallow traps, whose concentration was calculated using the positron trapping model in good agreement with that measured using the Hall effect.

Coincidence Doppler-broadening measurements showed the presence of copper in the vicinity of the detected vacancy-like defects. Thus, we believe that the observed vacancy-type defects are bound to Cu impurities or vice versa. This is supported by the theoretical calculation of the momentum distribution, which predicted the trapping of positrons to $V_{\text{Ga}}\text{-Cu}_{\text{Ga}}$ complexes.

ACKNOWLEDGMENTS

The authors are grateful for the valuable help of H. Mähl for Cu deposition. We would like to thank U. Kretzer and S. Eichler (Freiberger Compound Materials GmbH) for performing Hall measurements and supplying the sample materials. Financial support from the Egyptian Higher Education Ministry and Minia University for conducting this study in Germany is gratefully acknowledged.

*melabdalla@yahoo.co.uk

¹R. C. Newman, *Semicond. Sci. Technol.* **9**, 1749 (1994).

²D. T. J. Hurle, *J. Phys. Chem. Solids* **40**, 613 (1979).

³T. Y. Tan, U. Gösele, and S. Yu, *Crit. Rev. Solid State Mater. Sci.* **17**, 47 (1991).

⁴T. Y. Tan, H. M. You, and U. M. Gösele, *Appl. Phys. A: Solids Surf.* **56**, 249 (1993).

⁵G. A. Baraff and M. Schlüter, *Phys. Rev. B* **33**, 7346 (1986).

⁶D. J. Chadi, *Mater. Sci. Forum* **258-263**, 1321 (1997).

⁷E. W. Williams, *Phys. Rev.* **168**, 922 (1968).

- ⁸C. Domke, P. Ebert, M. Heinrich, and K. Urban, *Phys. Rev. B* **54**, 10288 (1996).
- ⁹R. Krause-Rehberg and H. S. Leipner, *Positron Annihilation in Semiconductors* (Springer, Berlin, 1999).
- ¹⁰P. Hautojärvi, *Positrons in Solids*, Vol. 12 of Topics in Current Physics, edited by P. Hautojärvi (Springer, Heidelberg, 1979).
- ¹¹K. G. Lynn, *Positron Solid State Physics*, edited by W. Brandt and A. Dupasquier (North-Holland, Amsterdam, 1983), p. 609.
- ¹²P. Hautojärvi and C. Corbel: *Positron Spectroscopy of Solids*, in *Proceedings of the Int. School of Physics, Enrico Fermi* (ISO Press, Amsterdam, 1995), p. 491.
- ¹³C. Corbel and P. Hautojärvi: *Positron Spectroscopy of Solids*, in *Proceedings of the Int. School of Physics, Enrico Fermi* (ISO Press, Amsterdam, 1995), p. 533.
- ¹⁴R. Krause-Rehberg, H. S. Leipner, T. Abgarjan, and A. Polity, *Appl. Phys. A* **66**, 599 (1998).
- ¹⁵M. J. Puska and R. M. Nieminen, *Rev. Mod. Phys.* **66**, 841 (1994).
- ¹⁶K. Saarinen, P. Hautojärvi, P. Lanki, and C. Corbel, *Phys. Rev. B* **44**, 10585 (1991).
- ¹⁷R. Krause-Rehberg, H. S. Leipner, A. Kupsch, A. Polity, and Th. Drost, *Phys. Rev. B* **49**, 2385 (1994).
- ¹⁸S. Fujii and S. Tanigawa, *Hyperfine Interact.* **79**, 719 (1993).
- ¹⁹M. Alatalo, H. Kauppinen, K. Saarinen, M. J. Puska, J. Mäkinen, P. Hautojärvi, and R. M. Nieminen, *Phys. Rev. B* **51**, 4176 (1995).
- ²⁰P. Asoka-Kumar, M. Alatalo, V. J. Ghosh, A. C. Kruseman, B. Nielsen, and K. G. Lynn, *Phys. Rev. Lett.* **77**, 2097 (1996).
- ²¹H. Kauppinen, L. Baroux, K. Saarinen, C. Corbel, and P. Hautojärvi, *J. Phys.: Condens. Matter* **9**, 5495 (1997).
- ²²J. Gebauer, M. Lausmann, T. E. M. Staab, R. Krause-Rehberg, M. Hakala, and M. J. Puska, *Phys. Rev. B* **60**, 1464 (1999).
- ²³K. Saarinen, P. Hautojärvi, A. Vehanen, R. Krause, and G. Dlubek, *Phys. Rev. B* **39**, 5287 (1989).
- ²⁴P. J. Schultz, K. G. Lynn, I. K. Mackenzie, Y. C. Jean, and C. L. Snead, *Phys. Rev. Lett.* **44**, 1629 (1980).
- ²⁵S. Linderroth and C. Hidalgo, *Phys. Rev. B* **36**, 4054 (1987).
- ²⁶L. C. Smedskjaer, M. Manninen, and M. J. Fluss, *J. Phys. F* **10**, 2237 (1980).
- ²⁷I. K. Mackenzie, *Phys. Rev. B* **16**, 4705 (1977).
- ²⁸M. J. Puska, O. Jepsen, O. Gunnarsson, and R. M. Nieminen, *Phys. Rev. B* **34**, 2695 (1986).
- ²⁹G. Dlubek, O. Brümmer, F. Plazaola, and P. Hautojärvi, *J. Phys. C* **19**, 331 (1986).
- ³⁰S. Dannefear and D. Kerr, *J. Appl. Phys.* **60**, 591 (1986).
- ³¹P. Hautojärvi, P. Moser, M. Stucky, C. Corbel, and F. Plazaola, *Appl. Phys. Lett.* **48**, 809 (1986).
- ³²M. Elsayed, V. Bondarenko, K. Petters, J. Gebauer, and R. Krause-Rehberg, *J. Appl. Phys.* **104**, 103526 (2008).
- ³³T. Laine, K. Saarinen, J. Mäkinen, P. Hautojärvi, C. Corbel, L. N. Pfeiffer, and P. H. Citrin, *Phys. Rev. B* **54**, R11050 (1996).
- ³⁴M. Alatalo, B. Barbiellini, M. Hakala, H. Kauppinen, T. Korhonen, M. J. Puska, K. Saarinen, P. Hautojärvi, and R. M. Nieminen, *Phys. Rev. B* **54**, 2397 (1996).
- ³⁵T. Hiramoto and T. Ikoma, *The Source of Copper Contamination in Commercial Semi-insulating GaAs Wafers*, Semi-insulating III-V Materials, Malmö Sweden, 1988, edited by G. Grossmann and L. Ledebro (Adam Hilger, Bristol, UK, 1988), p. 337.
- ³⁶H. S. Leipner, R. F. Scholz, F. Syrowatka, J. Schreiber, and P. Werner, *Philos. Mag. A* **79**, 2785 (1999).
- ³⁷R. N. Hall and J. H. Racette, *J. Appl. Phys.* **35**, 379 (1964).
- ³⁸R. A. Roush, D. C. Stoudt, and M. S. Mazzola, *Appl. Phys. Lett.* **52**, 2670 (1993).
- ³⁹R. Leon, P. Werner, K. M. Yu, M. Kaminska, and E. R. Weber, *Appl. Phys. A* **61**, 7 (1995).
- ⁴⁰N. A. Gokcen, *Bull. Alloy Phase Diagrams* **10**, 11 (1989).
- ⁴¹J. Kansy, *Nucl. Instr. Meth. A* **374**, 235 (1996).
- ⁴²J. Kansy, LT for Windows, Version 9.0, Inst. of Phys. Chem. Of Metals, Silesian University, Bankowa 12, PL-40-007 Katowice, Poland, March 2002 (private communication).
- ⁴³A. Sen Gupta, S. V. Naidu, and P. Sen, *Appl. Phys. A* **40**, 95 (1986).
- ⁴⁴R. Krause-Rehberg, K. Petters, and J. Gebauer, *Physica B* **273-274**, 714 (1999).
- ⁴⁵F. Börner, S. Eichler, A. Polity, R. Krause-Rehberg, R. Hammer, and M. Jurisch, *Appl. Surf. Sci.* **149**, 151 (1999).
- ⁴⁶V. Bondarenko, K. Petters, R. Krause-Rehberg, J. Gebauer, and H. S. Leipner, *Physica B* **308-310**, 792 (2001).
- ⁴⁷R. Krause-Rehberg and H. S. Leipner, *Appl. Phys. A: Mater. Sci. Process.* **64**, 457 (1997).
- ⁴⁸J. Gebauer, R. Krause-Rehberg, C. Domke, P. Ebert, and K. Urban, *Phys. Rev. Lett.* **78**, 3334 (1997).
- ⁴⁹T. E. M. Staab, M. Haugk, A. Sieck, Th. Frauenheim, and H. S. Leipner, *Physica B* **273-274**, 501 (1999).
- ⁵⁰M. Puska and R. Nieminen, *J. Phys. F: Metal Phys.* **13**, 333 (1983).
- ⁵¹C. Le Berre, C. Corbel, K. Saarinen, S. Kuisma, P. Hautojärvi, and R. Fornari, *Phys. Rev. B* **52**, 8112 (1995).
- ⁵²K. Petters, J. Gebauer, F. Redmann, H. S. Leipner, and R. Krause-Rehberg, *Mater. Sci. Forum* **363-365**, 111 (2001).
- ⁵³B. Barbiellini, M. J. Puska, T. Korhonen, A. Harju, T. Torsti, and R. M. Nieminen, *Phys. Rev. B* **53**, 16201 (1996).
- ⁵⁴M. Elsayed, V. Bondarenko, K. Petters, and R. Krause-Rehberg, *J. Phys.: Conf. Series* **265**, 012005 (2011).
- ⁵⁵M. Manninen and R. M. Nieminen, *Appl. Phys. A* **26**, 93 (1981).
- ⁵⁶B. Pagh, H. E. Hansen, B. Nielsen, G. Trumphy, and K. Petersen, *Appl. Phys. A* **33**, 255 (1984).
- ⁵⁷N. W. Ashcroft and N. D. Mermin, *Solid State Physics* (Holt-Saunders, New York, 1976), p. 579.
- ⁵⁸O. V. Boev, M. J. Puska, and R. M. Nieminen, *Phys. Rev. B* **36**, 7786 (1987).
- ⁵⁹J. Gebauer, M. Lausmann, F. Redmann, R. Krause-Rehberg, H. S. Leipner, E. R. Weber, and P. Ebert, *Phys. Rev. B* **67**, 235207 (2003).